ARTICLES

Mobility in Maltose−Water Glasses Studied with ^{1}H NMR

Ivon J. van den Dries,[†] Dagmar van Dusschoten,[‡] and Marcus A. Hemminga*[,‡]

Department of Food Science, Food Physics Group, Wageningen Agricultural University, P.O. Box 8129, 6700 EV Wageningen, The Netherlands, and Department of Molecular Physics, Wageningen Agricultural University, P.O. Box 8128, 6700 ET Wageningen, The Netherlands

Received: June 22, 1998; In Final Form: September 25, 1998

We have studied the molecular mobility of the water and carbohydrate protons in maltose samples as a function of water content and temperature using ^{1}H NMR. In the NMR signal, slow decaying and fast decaying fractions of protons are distinguished as arising from mobile and immobile ($\tau_c > 3$ μs) protons, respectively. The assignment of these fractions in terms of water and maltose protons is temperature dependent. By analyzing the relaxation behavior of the mobile protons, the mobility of the water molecules is determined. The mobility of water molecules increases with water content and temperature, and at the glass transition, a small break in mobility is observed, indicating that the water molecules slightly sense the glass transition. The method of second moments gives information about the mobility of the immobile protons. Upon cooling, the glass transition is marked by a decrease in the temperature dependence of the mobility of the hydroxyl protons of maltose. This suggests that a stable hydrogen-bond network between the sugar molecules is formed at the glass transition temperature that immobilizes the hydroxyl groups. Water disrupts this network, and this results in a higher mobility of the hydroxyl protons of maltose. The more water the stronger is this plasticizing effect.

Introduction

During the last few years there has been an increasing interest in the study of molecular motions in glassy food materials.[1] Discontinuities in macroscopic properties such as the viscosity, specific heat, and specific volume characterize the glass transition. At a molecular level, an interpretation of these macroscopic discontinuities is still lacking, but the macroscopic changes must be related to a change of molecular mobility. Several techniques can be used to study molecular mobility around the glass transition temperature such as electron spin resonance (ESR),[2−4] fluorescence,[5,6] dielectric relaxation,[7] and nuclear magnetic resonance (NMR) techniques.[8−11] From these studies, it is clear that although the mobility of the glass-forming molecules decreases strongly around the glass transition temperature, small molecules such as fluorescent or spin probes remain relatively mobile.[2−5,8,9,12−16]

In the present work, we focus on the molecular mobility in maltose−water systems. It is known that water reorients relatively independent of the carbohydrate matrix,[9] resembling other small molecules in a matrix. Although water molecules only slightly sense the glass transition of the matrix, their presence largely depresses the glass transition temperature. The molecular mechanism of this plasticizing effect is studied with proton NMR. With NMR, immobile ($\tau_c > 13$ μs) and mobile protons are distinguished and can be roughly assigned to hydroxyl and ring protons of maltose and water. By analysis of the relaxation behavior of the mobile protons, the mobility of the water is studied. The method of second moments is used to obtain information about the mobility of the immobile protons around the glass transition temperature. On the basis of the results of mobility of protons around the glass transition temperature, a molecular mechanism of plasticization is proposed.

Materials and Methods

Preparation of Maltose−Water Samples. Maltose monohydrate (Merck) was mixed with the appropriate amount of water in a 5 mm NMR tube to adjust the content of maltose to 80, 90, and 93 wt %. For the 95 wt % sample, maltose monohydrate was used without addition of water. The NMR tubes were sealed to prevent water evaporation. The maltose−water samples were melted in an oil bath at a temperature of about 420 K. The melting time was as short as possible to obtain a homogeneous melted sample without browning by degradation of the maltose. Melted maltose samples were quickly cooled and stored below their respective glass transition temperature. Maltose with deuterated hydroxyl groups was prepared by dissolving the monohydrate (1 g) in D_2O (5 mL) and subsequently freeze-drying before adjusting the water content with D_2O. The glass transition temperature of the deuterated samples was measured with differential scanning calorimetry (DSC) and compared with literature values.[7] The D_2O contents were 7 and 21 wt %.

NMR Spectroscopy. ^{1}H NMR measurements were performed on a Bruker AMX 300 spectrometer equipped with a Bruker 5

* To whom correspondence should be addressed.
[†] Wageningen Agricultural University.
[‡] Wageningen Agricultural University.

10.1021/jp982718v CCC: $15.00
Published on Web 12/01/1998

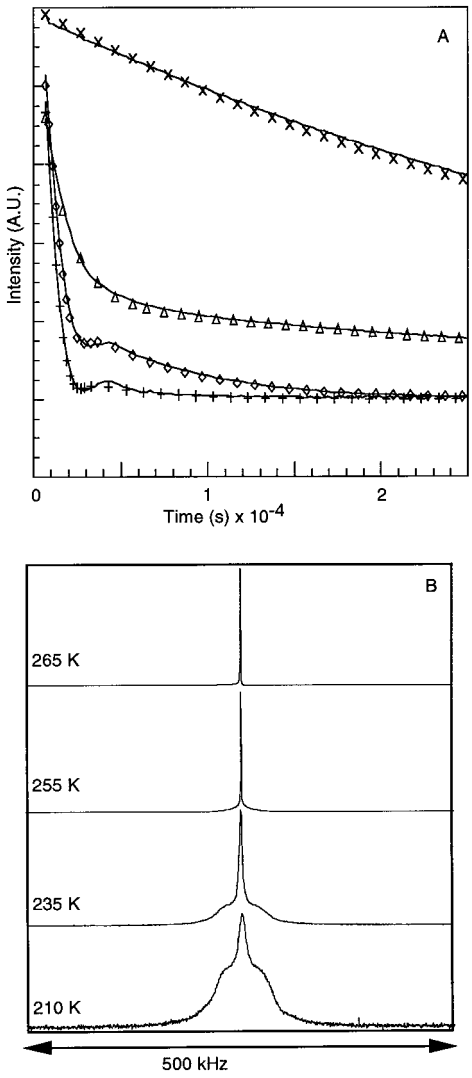

Figure 1. Free induction decays (FIDs) of 80 wt % maltose−water samples (A) and the corresponding Fourier transformed NMR spectra (B). For temperatures below 250 K, the experimental FIDs are fitted to eq 1, whereas at higher temperatures a biexponential function is used. The fits are indicated by (+) 210, (◇) 235, (△) 255, and (X) 265 K. The FIDs are scaled to the value of fit parameters $A + B$, and the NMR spectra are scaled to the intensity of the highest peak.

mm proton probe operating at a resonance frequency of 300.13 MHz. The temperature was regulated with a nitrogen temperature control. In this way, the temperature stability was within ±0.5 K. A spectral width of 500 kHz was used. The duration of the 90° pulse was 6−7 μs. The presented free induction decays (FID) are averages of eight scans having 2048 data points. Cross relaxation rates were measured with the Goldman Shen pulse sequence.[17,18] This pulse sequence of three $90_x°$ pulses makes use of the difference in spin−spin relaxation between fast and slow relaxing protons.

For the analysis of the NMR data at low temperatures, the FIDs $F(t)$ were fitted to the following equation:

$$F(t) = A \exp\left[-\frac{a^2t^2}{2}\right]\frac{\sin bt}{bt} + B \exp\left[\frac{-t}{T_{2m}}\right] \qquad (1)$$

In this equation, the parameters A and B represent the contributions of the immobile and mobile protons in the sample, also presented by the integral of the broad and sharp line shape parts of the NMR spectrum, respectively (see parts A and B of Figure 1). Parameter T_{2m} is the spin−spin relaxation time of the mobile proton fraction. The NMR spectrum of the immobile proton fraction is assumed to be a rectangular line shape with a total width $2b$, convoluted with a Gaussian line shape with a standard deviation given by parameter a.[19,20]

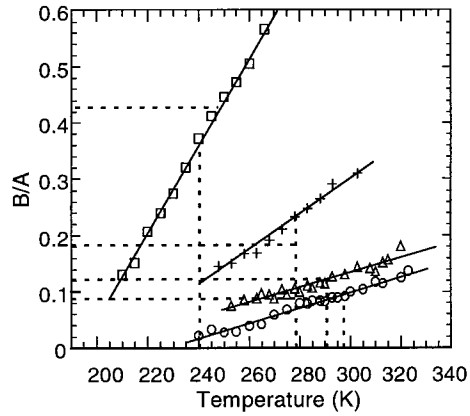

Figure 2. The ratio of the mobile (B) and immobile (A) proton fractions as a function of temperature for 95 (○), 93 (△), 90 (+), and 80 wt % (□) maltose samples. The straight lines are linear fits through the data points. The glass transition temperatures are indicated with dashed vertical lines. The dashed horizontal lines indicate the calculated values of B/A from Table 1.

For a resonance curve described by a normalized shape function $f(\omega)$ with a maximum at a frequency ω_0, the second moment M_2 with respect to the point ω_0 is defined as:[19]

$$M_2 = \int (\omega - \omega_0)^2 f(\omega)\, \partial\omega \qquad (2)$$

In our systems, the second moment is not used for the whole system but only for the broad part of the line shape that arises from the immobile proton fraction. The second moment M_2 of the broad line shape, which is a measure of the strength of the dipolar interactions, is calculated from the fit parameters a and b by the following equation:[19]

$$M_2 = a^2 + \frac{1}{3}b^2 \qquad (3)$$

On increasing the temperature, the dipolar interactions start to average and the broad component of the NMR spectrum sharpens up. As long as the FIDs show oscillations, characteristic for the rectangular line shape of the immobile proton fraction, they are well fitted by eq 1. Finally, the oscillatory character of the FID is lost, and the FIDs are fitted to a biexponential function.

Results

The FIDs of a 80 wt % maltose−water sample at various temperatures are shown in Figure 1A, and the corresponding NMR spectra are shown in Figure 1B. The NMR spectra at low temperature consist of a sharp line shape, arising from relatively mobile protons, superimposed on a broad line shape, arising from immobile protons. The ratio of the mobile (B) and immobile (A) proton fractions in various maltose−water samples, as determined from fitting the FID to eq 1, is shown versus temperature in Figure 2. For all samples, the ratio B/A increases almost linearly with increasing temperature, indicating that protons gradually go over from the immobile to the mobile fraction. No breaks are observed at the glass transition temperatures T_g,[7] which are indicated by the vertical lines in Figure 2. With increasing water content, the slope of the lines increases.

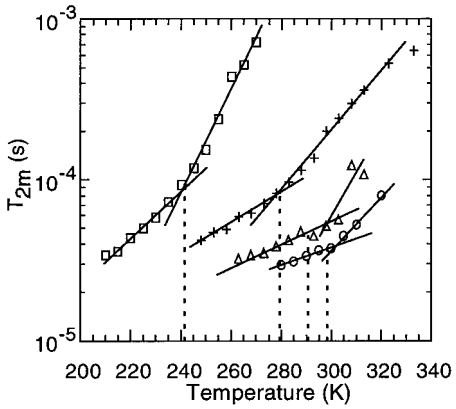

Figure 3. The relaxation time of the mobile protons (T_{2m}) versus temperature for 95 (○), 93 (△), 90 (+), and 80 wt % (□) maltose samples. The straight lines are linear fits through the data points. The glass transition temperatures are indicated with dashed vertical lines.

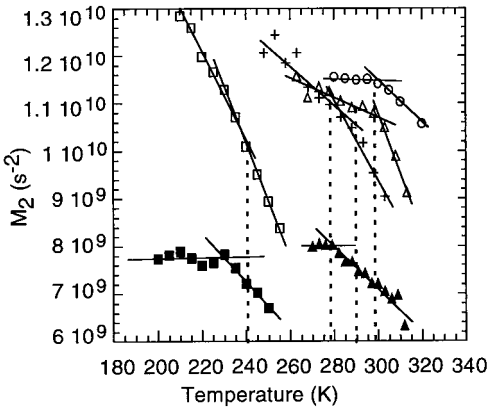

Figure 4. The second moment of the immobile protons (M_2) versus temperature for 95 (○), 93 (△), 90 (+), and 80 wt % (□) maltose samples. The second moment of solid protons in deuterated samples (93 and 79 wt %) is shown with corresponding filled symbols. The straight lines are linear fits through the data points. The glass transition temperatures are indicated with dashed vertical lines.

For the 80 wt % maltose−water sample at a temperature of 255 K (Figure 1), the typical characteristic of the broad line shape has completely disappeared and both line shape contributions have strongly sharpened up. In this case, eq 1 can no longer be used for the analysis of the FID and a biexponential fit is used instead. All data shown are fitted to eq 1, except for the samples with 80 wt % maltose at temperatures higher than 250 K and for the samples with 90 wt % maltose at temperatures above 300 K.

The spin−spin relaxation time of the mobile protons, T_{2m}, obtained from the analysis of the FIDs, is plotted in Figure 3. In all cases, an increase of T_{2m} is observed at higher temperatures and water contents, resulting in a sharpening of the line shape of the mobile protons. Also, in this figure a rapid increase occurs in T_{2m} around T_g, indicated by the vertical lines. It is remarkable that T_{2m} at T_g increases with increasing water content, resulting in a sharper line shape, although the temperature decreases.

From the parameters a and b deduced from the fits of the FIDs with eq 1, the second moment M_2 of the broad line shape is calculated using eq 3. For samples with a low water content, the values of the second moment were also calculated using the integral method (eq 2) to check the validity of eq 3. The values of M_2 were comparable, and therefore, all data on M_2 of the immobile fraction are obtained with eq 3. The results are shown in Figure 4 as a function of water content and temperature for protonated as well as for deuterated maltose−water systems. Higher values of M_2 are observed for the protonated samples (open symbols) as compared to the deuterated samples (filled symbols). Around the glass transition temperature T_g, indicated with vertical lines, breaks in M_2 are observed. Below T_g, a plateau value of M_2 is reached in both deuterated samples and the protonated 95 wt % maltose−water sample. In the other protonated samples, the increase of M_2 with decreasing temperature below T_g is larger if the sample contains more water. Below T_g, higher values of M_2 are reached on increasing water contents.

The cross relaxation rates in maltose−water systems, as determined with the Goldman Shen pulse sequence,[17,18] are on the order of 10^3 s^{-1}. The cross relaxation rates slightly decrease with temperature and water content.

Discussion

In this paper, it is our aim to investigate the physical state and dynamics of the water and maltose molecules in concentrated maltose−water samples using ^{1}H NMR. The water content

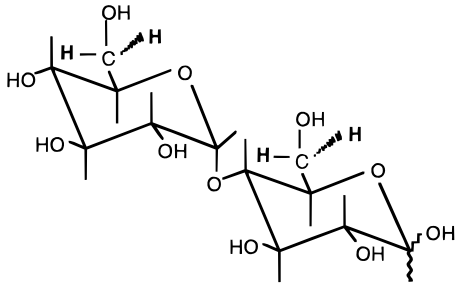

Figure 5. Molecular structure of maltose. The eight hydroxyl protons (plain) and the four exocyclic protons (bold) are shown.

ranges between 5 and 20 wt % water. This corresponds to an average number of water molecules per maltose molecule in the range 1−4.75, respectively. Under these conditions, all water molecules are unfreezable. The chemical structure of maltose is shown in Figure 5. The protons of maltose can be divided in three groups: ten protons directly bound to the glucose rings, four CH_2 protons of the exocyclic groups, and eight hydroxyl protons. The mobility of the ring protons is thought to follow the overall mobility of the maltose molecule as a whole. The CH_2 and hydroxyl protons may have a higher albeit restricted mobility because they are remote from the ring and therefore have an additional degree of motional freedom. Furthermore, the hydroxyl protons have the ability to exchange with the water protons and to form hydrogen bonds with the water molecules and with other OH groups.

To discuss the dynamics of the water and sugar protons, it is desirable to know which part of the ^{1}H NMR signal decay can be ascribed to the water and which part to maltose protons. In the free induction decay (FID), slow decaying and fast decaying fractions of protons are arising from mobile and immobile protons, respectively. In the following, the assignment of the slow and fast decaying part of the FID to water and sugar protons will be considered first, followed by a discussion of the transverse relaxation behavior (T_{2m}) of the mobile protons. Finally the second moment (M_2) of the immobile protons is discussed.

In Figure 1B, typical examples of low-temperature ^{1}H NMR spectra are shown for an 80 wt % maltose−water sample. The broad spectral component arises from immobile protons, and the relatively sharp peak, which is superimposed on it, arises from the mobile protons. The broad spectral component is the result of a distribution of static unaveraged proton dipole−dipole

TABLE 1: Molecular Ratio of Water and Maltose, Calculated Ratio B/A $(B/A)_{calc}$ Based on Proton Densities of Water and Maltose, Temperature (T_{calc}) Where this Value of B/A is Measured, and Glass Transition Temperature (T_g) for Various Maltose−Water Samples

wt % maltose	water/maltose	$(B/A)_{calc}$	T_{calc} (K)	T_g (K)
80	4.75	0.43	248	242
90	2.11	0.19	269	278
93	1.43	0.13	297	292
95	1.00	0.09	300	297

interactions in the sample. This results in a oscillatory behavior of the FID, where the frequency of the oscillations is a measure of the strength of the dipole interactions. The first part of the FID is then described by the damped sinusoidal part of eq 1. A similar FID was fitted using an equation in which the Gaussian part of eq 1 was replaced by an exponential.[11] Comparing both fits, we found that residual plots of the FID are best when using eq 1. The sharp line shape is well described by a Lorentzian line shape, characterized by a width at half-height given by $\Delta = (\pi T_{2m})._{-1}$ The lower limiting value of T_{2m} to describe the line shape with this equation is 2×10^{-5} s, which is about the width of the broad spectral component (Figure 1). This corresponds to an upper limit of the correlation time τ_c of 3×10^{-6} s calculated using the Bloembergen−Purcell−Pound theory.[19] Protons with τ_c values above 3×10^{-6} s will be part of the broad line shape and will be called immobile or solid in the following discussion.

^{1}H NMR signals of carbohydrate−water mixtures studied previously were divided into a slowly relaxing part and a fast relaxing part. The slowly relaxing fraction was often identified as originating from the water protons and the fast relaxing fraction from the carbohydrate protons, although it was noted that hydroxyl protons of the sugar could contribute to the slowly relaxing decay by chemical exchange.[9,11,21−23] Recently, it was observed in 93 wt % starch−water mixtures that some water molecules were relaxing fast at subzero temperatures.[24] This indicates that the immobile and mobile protons cannot be simply assigned to carbohydrate and water protons, respectively. This is also illustrated in Figure 2, which shows that the ratio of amplitudes of the mobile (B) and immobile (A) fractions (eq 1) is temperature dependent.

The ratio of water protons and maltose protons can be calculated from the known weight percentages of water and maltose in the samples. For example, in an 80 wt % maltose sample, the ratio of water to maltose molecules is 4.75 and thus the ratio B/A is calculated to be $9.5{:}22 = 0.43$. As is seen in Figure 2, this value is reached at a temperature of 248 K (see Table 1). The results for the various maltose−water samples are summarized in Table 1. In this table, it can be noticed that the temperature at which the calculated ratio B/A ($(B/A)_{calc}$) is observed (indicated by the dashed horizontal lines in Figure 2), tends to follow the glass transition temperature T_g. At higher or lower temperatures, the ratio B/A deviates from $(B/A)_{calc}$. This occurs because the separation of the NMR signal by the fit procedure is not based on discrimination between maltose and water protons but on discrimination between mobile and immobile protons. This separation is temperature dependent because the molecular mobility is temperature dependent. Therefore, it is possible that we find that above T_g more "mobile" protons exist than we can account for on basis of the known water content, whereas below T_g we find less "mobile" protons than we can account for.

A higher than calculated value of the ratio B/A can be explained by maltose protons becoming mobile, although it has also been explained to arise from chemical exchange between the water and the maltose protons. Chemical exchange is exchange of protons of the water and the sugar by which magnetization is exchanged.[25,26] If chemical exchange times have the same time scale as T_{2m}, 10^{-5} s, this exchange can significantly influence the amplitudes of the mobile and immobile fractions. Although it was observed[27] that the chemical exchange time for 60 wt % glucose−water samples at room temperature is on the order of 10^{-2} s and thus too slow to influence the ratio B/A, we also measured cross relaxation rates to estimate the influence of the chemical exchange rate on the ratio B/A in 80−95 wt % maltose−water samples at low temperatures. Cross relaxation is the inter- and intramolecular transfer of magnetization of protons by chemical exchange and/or spin diffusion. These effects can be measured with the Goldman Shen pulse sequence.[17,18] In this pulse sequence, the difference in transverse relaxation between the immobile and the mobile protons is used to determine the cross relaxation between the mobile and immobile protons. The cross relaxation rate in maltose glasses decreases with temperature and water content because the more rigid a sample, the more efficient is the cross relaxation takes place (data not shown). For the temperature and water content range we used, the cross relaxation rate was on the order of 10^3 s^{-1}, which is similar to the value observed before.[11] The upper limit for chemical exchange rate is thus 10^3 s^{-1}, while the transverse relaxation rates are at least 50 times larger (Figure 3). Thus, chemical exchange is too slow to influence the amplitudes B and A. The higher than calculated value of the ratio B/A above T_g must therefore be explained by sugar protons becoming mobile.

Most likely, the exocyclic hydroxyl protons of the sugar first go over from the immobile to the mobile fraction when the temperature is increased, because they are most remote to the ring and have therefore a higher, albeit restricted, mobility. If, for example, the two exocyclic hydroxyl protons go over to fraction B in a 80 wt % maltose sample, the ratio B/A is 0.57, which is reached at 25 degrees above T_g. Within the temperature and water content range we studied, two to three sugar protons at most behave in a liquidlike way. As mentioned above, in previous studies it was suggested that the hydroxyl protons of sugar molecules can contribute to the mobile protons in ^{1}H NMR experiments via chemical exchange.[21−23,28] However, the hydroxyl protons contribute to the mobile fraction because these protons become mobile not because of chemical exchange. At temperatures below T_g, the contribution of the immobile protons is relatively too large, which means that some water protons are immobile. This is illustrated by the fact that in 80 wt % maltose, the ratio B/A is 0.18 in the case that half of the water protons are immobile. This point is reached at 220 K. Solid water protons were also observed in 93 wt % starch at low temperatures.[24]

The slope of B/A versus temperature is a measure of the amount of protons going over from the immobile to the mobile fraction per degree (Figure 2). Below T_g, the slope reflects the water protons becoming mobile. The slope of B/A versus temperature increases with water content, because the more water protons are present the more protons will become mobile per degree of temperature. The slope of B/A in a sample with 20 wt % water is therefore expected to be 4.75 times higher than in a sample with 5 wt % water. The increase in mobility of the protons with temperature is a gradual process, and T_g is not marked by any discontinuity or a change in the rate of this process (Figure 2). However, above T_g, where all water protons already are mobile, the slope reflects the OH groups of the sugar

TABLE 2: Temperature-Dependent Assignment of the Mobile (*B*) and Immobile (*A*) Fraction in Terms of Water and Sugar

T	A (immobile)	B (mobile)
$<T_g$	maltose + H_2O	H_2O
T_g	maltose	H_2O
$>T_g$	maltose	H_2O + maltose

becoming so mobile that they no longer belong to the solid fraction. The amount of maltose protons decreases with increasing water content, but the slope above T_g increases with water content. This indicates that the average maltose proton mobility is higher in a sample with 20 wt % water as compared to a sample with 5 wt % water.

By a linear extrapolation to lower temperatures, the ratio *B*/*A* becomes zero around 200 K. This means that then no water mobility would be observed by ^{1}H NMR. In cellulose, in which the water molecules have a similar molecular environment, it was also observed that water mobility vanishes around 190 K.[29] Only a highly mobile independent flipping of some water molecules still persisted. Water mobility observed with ^{1}H NMR in organic polymers also vanishes in the same temperature range (160−190 K).[30−33]

The temperature-dependent assignment of the mobile and immobile fraction to water and maltose protons is summarized in Table 2. Below T_g, the mobile fraction (on the average) is thought to consist of only water protons. It is important for the following discussion to keep in mind that the immobile fraction at temperatures below T_g consists of water and sugar protons and that at higher temperatures both sugar and water contribute to the mobile fraction.

In Figure 3, it can be seen that in all samples the transversal relaxation time T_{2m} of the mobile fraction increases with increasing temperature. A small break in T_{2m} is observed at the glass transition temperature T_g. This indicates an additional increase in reorientational motions of the mobile water protons at T_g. From the dependence on water content, it can be seen that the fewer water molecules per maltose molecule, the stronger the water molecules sense the glass transition. This shows that at lower water contents the water molecules tend to have stronger interactions with the maltose molecules. The value of T_{2m} of about 10^{-4} s in maltose samples around T_g is a factor of 10^5 smaller than the T_2 of free water. The value of τ_c of water in maltose glasses is thus expected to be 10^{-7} s. This observation illustrates that water mobility is decoupled from the viscosity of the sample, which increases by a factor of 10^{12}, while the rotational mobility of the water is only slowed by a factor of 10^5. This decoupling of mobility of small molecules from the matrix mobility has been observed before in a glassy matrix.[9,13,34−36] In epoxy resin[37,38] or poly(vinylpyrrolidone)[16] glasses, water mobility is even less retarded compared to free water, probably because these polymers are much more hydrophobic and cannot form multiple hydrogen bonds. Not only rotational mobility but also translational mobility of small molecules is decoupled from the matrix mobility.[13,15,39,40] In Ficoll, a sucrose-based polymer, the translational mobility of water as determined from desorption experiments is unaffected by the glass transition of the carbohydrate.[15] The translational mobility of water was also found to be decoupled by a factor of 10^7 from that of the carbohydrate matrix in concentrated maltose samples in the vicinity of T_g.[13,40]

On comparing T_{2m} at the glass transition temperatures of every water content, it can be seen that T_{2m} increases with increasing water content. The value of T_{2m} depends on dipole interactions and rotational mobility. The dipole interactions of water protons are mainly determined by the distance of the two protons of water and thus constant. Therefore, it follows that at T_g the water molecules in an 80 wt % maltose−water sample are more mobile as compared to water molecules in a 95 wt % maltose−water sample, even though the temperature T_g has decreased. Theoretically, T_{2m} increases with temperature by an increase in molecular mobility. Therefore, a lower value of T_{2m} is expected at a lower glass transition temperature T_g. Such an effect is observed, for example, in a series of malto-oligomer samples with constant water content in which the chain length is varied.[9] However, for our maltose−water samples, this is not the case, and it can be concluded that the effect of water content on the rotational mobility exceeds the effect of temperature.

Clearly, increasing the water content reduces the molecular interactions between water and maltose protons and thus increases the rotational mobility. It is likely that in these highly concentrated maltose−water samples the water molecules mostly interact with the hydroxyl groups of the sugar.[41] A water molecule in a 95 wt % maltose sample hardly interacts with other water molecules in the time that the NMR signal decays. This can be calculated from the equation $x = (2Dt)^{1/2}$, in which x is the displacement and t the time. The diffusion coefficient D is 10^{-14} m^2/s in a 95 wt % sample at its glass transition temperature.[13,40] In such a maltose sample, having only one water molecule per maltose molecule, the calculated displacement of a water molecule (0.5 nm) during the time the NMR signal decays (around 10^{-5} s, the value of T_2) is on the same order of magnitude as the size of a maltose molecule. Thus, the water molecules in a 95 wt % maltose sample do not interact with other water molecules but will only form hydrogen bonds with maltose hydroxyl protons. On increasing the water content, more hydrogen bonds are formed between the water molecules, and this leads to an increase in motion and thus longer T_{2m} values. From the relaxation behavior of the mobile protons, it can be concluded that the rotational motion of the water molecules is decoupled from the mobility of the maltose molecules, as expected. However, at low water contents, the water molecules strongly interact with the maltose molecules and therefore sense the glass transition.

Having discussed the relaxation of the mobile protons, we proceed with the discussion of the immobile protons. The part of the FID originating from the immobile protons cannot be characterized by a T_2 value, and therefore the method of second moments is used.[19] This method was employed already in earlier studies of mobility in crystalline sugars[42,43] and glucose pentaacetate.[44]

The variation of the second moment M_2 of the immobile protons with temperature is shown in Figure 4. In the analysis of M_2, the following points should be taken into account.

1. A reduction of M_2 takes place if the proton density in the sample is lowered, because dipolar interactions decrease with the sixth power of the distance between protons.

2. M_2 will be reduced by anisotropic mobility or slow isotropic rotations that partly average out the dipolar interactions.

A clear indication for the first effect is seen on comparing the deuterated and protonated maltose−water samples. Since the average distance between the protons increases in the deuterated samples and deuterons hardly contribute to the dipolar couplings because of their low gyromagnetic ratio, the second moment M_2 is reduced in deuterated samples. Furthermore, the increasing value of M_2 below T_g is explained by an increasing proton density, because the relative number of protons contributing to M_2 is increasing. Also, the temperature dependence of

M_2 is related to effect 1. From Figure 2, we concluded that upon decreasing the temperature below T_g more and more water protons become part of the immobile fraction. These protons increase the value of M_2 because they give rise to an increased static proton density and a concomitant decrease in apparent proton−proton distances. The more water protons that become immobile, the stronger the increase in M_2. Therefore, the slope of M_2 versus temperature is larger for 80 wt % maltose−water samples as compared to 95 wt % maltose−water samples below T_g.

Related to the amount of immobile water protons is the limiting value of M_2 that is reached at low temperatures, where all water protons are immobilized. This limiting value should be higher in an 80 wt % maltose−water sample than in a 95 wt % sample, because the effect of water is to reduce the proton−proton distances and thus to increase M_2. Although this limiting value is not reached in the temperature range studied, the higher values of M_2 in a 80 wt % maltose−water sample as compared to a 95 wt % sample support this reasoning (Figure 4). The value of M_2 around T_g in a 95 wt % maltose−water sample (1.15×10^{10} s^{-2}) is somewhat smaller than the value of M_2 in monohydrate crystalline maltose (1.23×10^{10} s^{-2})[42] calculated from the known X-ray structure.[45] The somewhat lower experimental value of M_2 may reflect some local motions of the water molecules[42] (effect 2).

On increasing the temperature, all protonated maltose−water samples show a break in M_2 just above T_g. This relatively steep decrease of M_2 cannot be explained by proton density arguments, because Figure 2 shows no discontinuities around T_g. Therefore, the increase in slope just above T_g must be explained by the onset of additional mobility of hydroxyl or nonexchangeable protons (effect 2) that reduces M_2 more strongly than was the case below T_g. In the deuterated samples, this discontinuity is not observed above T_g, but below T_g. Thus, the extra decrease of M_2 above T_g in protonated samples is not due to extra mobility of the nonexchangeable maltose protons but to mobility of hydroxy protons. The steep decrease in M_2 displayed by the deuterated samples does not coincide with T_g nor with the temperatures reported for β-relaxation (203 K for 80 wt % and 219 K for 93 wt % maltose samples[7]). This effect can be explained as follows. Starting at low temperature, the motion of the nonexchangeable protons will gradually increase on increasing the temperature. However, at low temperatures the anisotropic mobility of these protons is too slow to influence M_2. This is reflected in the horizontal plateau value of M_2. At a certain temperature, the motions start to reduce M_2, giving rise to the observed decrease. This temperature is not necessarily related to T_g. It is likely that at first instance the decrease will probably be due to librations of the protons of the exocyclic CH_2OD groups, because they are most remote to the ring and therefore have an additional degree of motional freedom. It should be noted, however, that the effect of the nonexchangeable groups will play a role in the protonated samples, but it is overshadowed by the relatively large contribution of the exchangeable hydroxyl protons.

On the basis of the M_2 results, we can conclude that around T_g the hydroxyl protons of the maltose molecules become mobile. This suggests that the hydrogen-bond network starts to "melt" at T_g. A similar effect was deduced from molecular dynamics simulations.[46,47] Here, T_g is found to indicate an abrupt change in the hydrogen-bond properties (lifetime × number of hydrogen bonds), and upon heating, a weakening of the hydrogen-bond network is observed. Also neutron-scattering experiments with glassy glucose showed that the hydrogen network becomes less pronounced on heating and that the glass transition is accompanied by a decrease in the number of hydrogen bonds.[48]

The mobility of the hydroxyl protons also explains why the value of M_2 at T_g decreases with water content. The value of M_2 is higher for a protonated 93 wt % maltose−water sample as compared to a 80 wt % sample, while in deuterated samples there is no such difference in M_2 at T_g. Therefore, the decrease of M_2 at T_g with increasing water content must be due to mobility of the water or hydroxyl protons. Because at T_g all water protons belong to the mobile fraction (Table 2), we conclude that the lower value of M_2 at T_g with increasing water content is due to more mobile hydroxyl protons. Thus, the main effect of adding water is not an increase of water mobility but its effect on the maltose. The presence of water enhances the mobility of hydroxyl protons of maltose. If the mobility of the glass-forming molecules is large, the sample has to be cooled to a lower temperature before a glass is formed. This plasticization mechanism is similar to that in polymer glasses where plasticizers increase the mobility of side chains of the polymer. Water in polyvinyl alcohol is said to provide a lubrication effect that promotes chain mobility and disrupts hydrogen bonding, removing further barriers to bond rotation and chain mobility.[49]

On the basis of our results, we propose the following model for the molecular mobility in low water content maltose−water samples. The mobility of water and maltose protons decreases with decreasing water content and temperature. The glass transition is marked by a decrease in the temperature dependence of mobility of the hydroxyl protons of maltose. As a result of strong interactions between the maltose and water protons at low water contents, the water molecules also sense the glass transition. This suggests that upon cooling a stable hydrogen-bond network between the sugar molecules is formed at the glass transition temperature, which immobilizes the hydroxyl groups. Water molecules weaken this network, which results in a higher mobility of the hydroxyl protons of maltose. The more water, the stronger this plasticising effect. This property of water also explains why samples with a higher water content have to be cooled to lower temperatures before a glass is formed.

Acknowledgment. This research was partly supported by European Union Contract ERBFAIRCT961085. We thank S. Moolenaar for assistance with the NMR experiments.

References and Notes

(1) Roos, Y. *Phase Transitions in Foods*; Academic Press: San Diego, 1995.
(2) Roozen, M. J. G. W.; Hemminga, M. A. *J. Phys. Chem.* **1990**, *94*, 7326−7329.
(3) Roozen, M. J. G. W.; Hemminga, M. A.; Walstra, P. *Carbohydr. Res.* **1991**, *215*, 229−237.
(4) Roozen, M. J. G. W.; Hemminga, M. A. *Spec. Publ.—R. Soc. Chem.* **1991**, *82*, 531−536.
(5) Cicerone, M. T.; Blackburn, F. R.; Ediger, M. D. *J. Chem. Phys.* **1995**, *102*, 471−479.
(6) Cicerone, M. T.; Ediger, M. D. *J. Chem. Phys.* **1996**, *104*, 7210−7218.
(7) Noel, T. R.; Parker, R.; Ring, S. G. *Carbohydr. Res.* **1996**, *282*, 193−206.
(8) Diehl, R. M.; Fujara, F.; Sillescu, H. *Europhys. Lett.* **1990**, *13*, 257−62.
(9) Ablett, S.; Darke, A. H.; Izzard, M. J.; Lillford, P. J. *Studies of the glass transition in malto-oligomers*; Nottingham University Press: Nottingham, 1993.
(10) Girlich, D.; Lüdemann, H. D.; Buttersack, C.; Buchholz, K. *Z. Naturforsch. C* **1994**, *49*, 696.
(11) Hills, B. P.; Pardoe, K. *J. Mol. Liq.* **1995**, *63*, 229−237.
(12) Ediger, M. D.; Angell, C. A.; Nagel, S. R. *J. Phys. Chem.* **1996**, *100*, 13200−13212.
(13) Parker, R.; Ring, S. G. *Carbohydr. Res.* **1995**, *273*, 147−55.

(14) Girlich, D.; Lüdemann, H.-D. *Z. Naturforsch* **1993**, *49*, 250−257.
(15) Aldous, B. J.; Franks, F.; Greer, A. L. *J. Mater. Sci.* **1997**, *32*, 301−308.
(16) Oksanen, C. A.; Zografi, G. *Pharm. Res.* **1993**, *10*, 791−9.
(17) Kenwright, A. M.; Packer, K. J. *Chem. Phys. Lett.* **1990**, *173*, 471−475.
(18) Goldman, M.; Shen, L. *Phys. Rev.* **1966**, *144*, 321−331.
(19) Abragam, A. *The principles of nuclear magnetism*; Clarendon Press: Oxford, 1961.
(20) McBrierty, V. J.; Packer, K. J. *Nuclear magnetic resonance in solid polymers*; Cambridge University Press: Cambridge, 1995.
(21) Kalichevsky, M. T.; Jaroszkiewicz, E. M.; Blanshard, J. M. V. *Polymer* **1993**, *34*, 346−58.
(22) Kalichevsky, M. T.; Jaroszkiewicz, E. M.; Ablett, S.; Blanshard, J. M. V.; Lillford, P. J. *Carbohydr. Polym.* **1992**, *18*, 77−88.
(23) Farhat, I. A.; Mitchell, J. R.; Blanshard, J. M. V.; Derbyshire, W. *Carbohydr. Polym.***1996**, *30*, 219−227.
(24) Li, S.; Dickinson, L. C.; Chinachoti, P. *J. Agric. Food Chem.* **1998**, *46*, 62−71.
(25) Edzes, H. T.; Samulski, E. T. *J. Magn. Reson.* **1978**, *31*, 207−229.
(26) Zimmerman, J. R.; Brittin, W. E. *J. Phys. Chem.* **1957**, *61*, 1328−1333.
(27) Hills, B. P. *Mol. Phys.* **1991**, *72*, 1099−1121.
(28) Ablett, S.; Izzard, M. J.; Lillford, P. J. *J. Chem. Soc., Faraday Trans.* **1992**, *88*, 789−794.
(29) Radloff, D.; Böffel, C.; Spiess, H. W. *Macromolecules* **1996**, *29*, 1528−1534.
(30) Coyle, F. M.; Martin, S. J.; McBrierty, V. J. *J. Mol. Liq.* **1996**, *69*, 95−116.
(31) McBrierty, V. J.; Zhang, X.; Douglass, D. C.; Zhang, J. X.; Jerome, R. *Polymer* **1994**, *35*, 3811−3815.
(32) Quinn, F. X.; Kampff, E.; Smyth, G.; McBrierty, V. J. *Macromolecules* **1988**, *21*, 3191−3198.
(33) Smyth, G.; Quinn, F. X.; McBrierty, V. J. *Macromolecules* **1988**, *21*, 3198−3204.
(34) Blackburn, F. R.; Cicerone, M. T.; Hietpas, G.; Wagner, P. A.; Ediger, M. D. *J. Non-Cryst. Solids* **1994**, *172*, 256−264.
(35) Blackburn, F. R.; Wang, C.; Ediger, M. D. *J. Phys. Chem.* **1996**, *100*, 18249−18257.
(36) Chang, I.; Fujara, F.; Geil, B.; Heuberger, G.; Mangel, T.; Sillescu, H. *J. Non-Cryst. Solids* **1994**, *172*, 248−255.
(37) Jelinski, L. W.; Dumais, J. J.; Stark, R. E.; Ellis, T. S.; Karasz, F. E. *Macromolecules* **1983**, *16*, 1019−1021.
(38) Jelinski, L. W.; Dumais, J. J.; Cholli, A. L.; Ellis, T. S.; Karasz, F. E. *Macromolecules* **1985**, *18*, 1091−1095.
(39) Champion, D.; Hervet, H.; Blond, G.; Le Meste, M.; Simatos, D. *J. Phys. Chem. B* **1997**, *101*, 10674−10679.
(40) Tromp, R. H.; Parker, R.; Ring, S. G. *Carbohydr. Res.* **1997**, *303*, 199−205.
(41) Girlich, D.; Lüdemann, H.-D. *Z. Naturforsch* **1993**, *48c*, 407−413.
(42) Reynhardt, E. C. *Mol. Phys* **1990**, *69*, 1083−1097.
(43) Reynhardt, E. C.; Latanowicz, L. *Chem. Phys. Lett.* **1996**, *251*, 235−241.
(44) Ellis, B.; McDonald, M. P. *J. Non-Cryst. Solids* **1969**, *1*, 186−94.
(45) Gress, M. E.; Jeffrey, G. A. *Acta Crystallogr.* **1977**, *B33*, 2490−2495.
(46) Caffarena, E.; Grigera, J. R. *J. Chem. Soc., Faraday Trans.* **1996**, *92*, 2285−2289.
(47) Caffarena, E. R.; Grigera, J. R. *Carbohydr. Res.* **1997**, *300*, 51−57.
(48) Tromp, R. H.; Parker, R.; Ring, S. G. *J. Chem. Phys.* **1997**, *107*, 6038−6049.
(49) Hodge, R. M.; Bastow, T. J.; Edward, G. H.; Simon, G. P.; Hill, A. J. *Macromolecules* **1996**, *29*, 8137−8143.